On the Use of Subcarriers in Future Space Missions

M. M. Shihabi, T. M. Nguyen and S. M. Hinedi.
April 6, 1983

Jet Propulsion Laboratory
California Institute of Technology
4800 Oak Grove Dr, MS 238-343
Pasadena, CA 91109

The performance of deep space telemetry signals that *employ a* residual carrier modulation technique is compared in the presence and absence *of* a *subcarrier.* When the *subcarrier* is present, *the* performance for the resulting pulse-coded modulation/phase-shift *keyed/phase-modulat* ed *(PCM/PSK/PM)* scheme is e *valu*ated for both sine wave and square wave *subcarriers* and non-return-to zero *(NRZ)* data. When the *subcarrier* is absent, the performance *for the resulting PCM/PM* technique is evaluated *for* both the *NRZ* and the *bi-phase* data format. The com*parison is* based on telemetry performance as well *as* bandwidth efficiency. The first criterion is characterized *in terms of the* symbol error rate *(SER) as* a *function of symbol* SNR, *loop bandwidth-to-data* rate ratio, and modulation index. *The band*width efficiency is characterized by *the occupancy* factor, The results *of* both the analysis and *measurements show that when the interference-to-carrier* ratio *(ICR) is less* than – 15 all?, *the performance degradation* in the absence *of a subcarrier* is negligible. Various combinations *of loop* bandwidth- *to-dat* a rate *ratios* and modulation indices that achieve this *performance* are derived and listed. Bandwidth *occupancy* comparison indicates that *PCM/PM/NRZ* is *the* mast efficient in this regard. Therefore, by eliminating the *subcarrier* and using the *PCM/PM/NRZ* scheme, many advantages can *be* realized without any sacrifice *in performance.*

* **The research described in this paper was carried out by the Jet Propulsion Laboratory, California Institute of Technology, under a** contract with the **National Aeronautics and Space Adrninistration.**

L Introduction

In the past when space missions operated at low data rates using residual carrier modulation, it was necessary to separate the data from the residual carrier to avoid interference. This was achieved by placing the data modulation on a subcarrier since direct modulation of the data on the carrier would cause moat of the data power to fall within the bandwidth of the carrier phase-lock loop (PLL) and, as a consequence, interfere with its operation [1, Chap. 3]. The scheme in which the data is phase-shift keyed (PSK) onto a subcarrier and then phase-modulated (PM) onto a sinusoidal carrier is called the PCM/PSK/PM modulation scheme. However, space missions and the Deep Space Network (DSN) supporting them have evolved over the years and will soon be capable of supporting very high data rates, on the order of tens of megabits per second [1, Chap. 3]. At these higher data ratea, the data signal spectrum is broad, and therefore, if the subcarrier were to be eliminated, the part of the spectrum that would fall within the carrier loop bandwidth would be flat and appear as white noise to a narrow loop. Since the ratio of loop bandwidth to data rate is very small at high data rates, it would seem that this additional white noise component would degrade the tracking performance very little. This later scheme in which the telemetry data are phase modulated directly onto the carrier is known as the PCM/PM modulation scheme.

In this paper, the use of residual carrier techniques with no subcarrier (PCM/PM) will be advocated. It will be shown that the use of the PCM/PM technique under appropriate conditions will reap many advantages without sacrificing performance. Foremost among these advantage is the lower bandwidth, which can be extremely useful when antenna arraying is employed or when tracking multiple spacecraft signals within the field of view of a single antenna, In the latter case, the various signals can be separated in the frequency domain and a single receiver front end can be used to downconvert them to baseband. This idea is very similar to frequency division multiplexing (FDM) except that the carriers are generated by different oscillators. Secondly, PCM /PM has the advantage of eliminating sub carrier loss in the receiver. Finally, the presence of the residual carrier provides useful data for navigation purposes and also safeguards the investment made in PLL receivers by the DSN and other space agencies. In light of the above, the goal of this article is the assessment and comparison of performance degradation in DSN receivers due to the interference between the data and the residual carrier in the above two schemes. For the PCM/PM modulation scheme, two kinds of data formats are considered. The non-return-to-zero (NRZ) format and the Manchester (or hi-phase) data format. For the PCM/PSK/PM modulation scheme, the performance is determined for the two moat commonly used subcarriers: the square wave, which is used for deep space missions (category B) and the sine wave, which is used for near-Earth missions (category A), as recommended by the Consultative Committee for Space Data Systems (CCSDS) [2]. The comparison

is based on the telemetry symbol error rate (SER) and the bandwidth (BW) occupancy. Throughout this article, it is assumed that the data are not encoded. Hence, the SER is equivalent to the bit error rate (BER), and the two terms are used interchangeably.

The paper is organized as follows: A brief description of the various residual carrier modulation schemes is presented in Section II. The general analysis and summary of the theoretical results are presented in Section 111. The discussion and comparison of theoretical and measured performance are carried out in Section IV, followed by the conclusion in Section V.

II. Description of the Residual Carrier Modulation Techniques

The telemetry signal in the two schemes can be represented mathematically by

$$s(t) = \sqrt{2P_T}\sin(\omega_c t + mP(t)d(t)) \tag{1}$$

where P_T is the total power; ω_c is the angular carrier frequency in rad/see; m is the modulation index in radians ($0 < m < \pi/2$); $d(t)$ is the binary data sequence with symbol rate $R_s = 1/T_s$; and

$$P(t) = \begin{cases} 1 & ; \text{PCM/PM} \\ \text{Sin}(\omega_{sc}t + \theta_{sc}) & ; \text{PCM/PSK/PM (square wave)} \\ \sin(\omega_{sc}t + \theta_{sc}) & ; \text{PCM/PSK/PM (sine wave)} \end{cases}$$

A. The PCM/PM Technique

There is no subcarrier used in this scheme, hence one substitutes 1 for $P(t)$ in Eq. (l), obtaining

$$s(t) = \sqrt{2P_T}\sin(\omega_c t + \text{red}(t)) \tag{2}$$

The received signal, $r(t)$, is corrupted by additive white Gaussian noise (AWGN), $n(t)$, with one-sided power spectral density N_0(W/Hz). By using simple trigonometric identities, the received signal can be expanded as

$$r(t) = \sqrt{2P_T}[\cos(m)\sin(\omega_c t + \theta_c) + d(t)\sin(m)\cos(\omega_c t + \theta_c)] + n(t) \tag{3}$$

where θ_c is the carrier phase. The first and second terms of Eq. (3) are the residual carrier components, $C(t)$, and the data components, $I_c(t)$, respectively. Explicitly,

$$C(t) = \sqrt{2P_T}\cos(m)\sin\ (\text{wet}+\ \theta_c) \tag{4a}$$

$$I_c(t) = \sqrt{2P_T}d(t)\sin\ (\text{m})\ \cos(\omega_c t + \theta_c) \tag{4b}$$

The data component is denoted by $I_c(t)$ to explicitly indicate its role as the interfering component to the carrier PLL. It is seen that the modulation index, m, has allocated the total transmitted power to the carrier and to the data channel, where the carrier power and data power are respectively given by

$$P_C = P_T \cos^2 m \tag{5a}$$

$$P_D = P_T \sin^2 m \tag{5b}$$

Another important parameter is the power spectral density (PSD) of the transmitted signal. From Eq. (2), it is easy to determine that the one-sided PSD of the transmitted signal in the PCM/PM scheme is equal to

$$S(f) = P_T[\cos^2(m)\delta(f - f_c) + \sin^2(m)S_D(f - f_c)] \tag{6}$$

where $S_D(f)$ is the PSD of the data sequence and is given by [1 ,4]

$$S_D(f) = \begin{cases} 1/R_s\ \dfrac{\sin^2(\pi f/R_s)}{(\pi f/R_s)^2}; & \text{NRZ data} \\ 1/R_s\ \dfrac{\sin^4(\pi f/2R_s)}{(\pi f/2R_s)^2}, & \text{bi-phase data} \end{cases} \tag{7}$$

By substituting in Eq. (6), one obtains expressions for the spectrum of the transmitted signal for these two cases, as shown in Fig. l(a) and l(b), respectively, Because of the symmetrical nature of the spectrum around the origin, only the posit ive frequency portion is shown in the graph.

B. The PCM/PSK/PM Technique

This scheme is the traditional residual carrier technique, where a subcarrier is used to separate the data from the carrier. The telemetry signal is given in Eq. (1) and results in

$$s(t) = \sqrt{2P_T}[\cos(mP(t))\sin(\omega_c t) + d(t)\sin(mP(t))\cos(\omega_c t)] \quad (8a)$$

where $d(t)$ is the NRZ binary data sequence, and $P(t)$ is the subcarrier waveform. Using Eq. **(8),** an expression for the PSD of the transmitted signal was derived in [5] for the two subcarrier waveforrna used in space applications. When $P(t)$ is a unit-power square-wave subcarrier of frequency f_{sc}, Eq. (8a) reduces to

$$s(t) = \sqrt{2P_T}[\cos(m)\sin(\omega_c t) + d(t)P(t)\sin(m)\cos(\omega_c t)] \quad (8b)$$

The power spectral density for this case is given by

$$S(f) = P_T\left\{\cos^2(m)\delta(f - f_c) + \left(\frac{4}{\pi^2}\right)\sin^2(m)\sum_{k>1}\left[[S_D(f - f_c - (2k-1)f_{sc}) + S_D(f - f_c + (2k-1)f_{sc})]/(2K-1)^2\right]\right\} \quad (9)$$

where $S_D(f)$ is the PSD of the NRZ binary data sequence which was defined earlier in Eq. (7). The first term in Eq. (9) is the residual carrier spectral component, and the second term is the data component. The plot of Eq. (9) is shown in Fig. l(c). The CCSDS recommends that the subcarrier frequency-to-bit rate, $n = f_{sc}/R_s$, be an integer [2] where R_s is the data rate. On the other hand, when $P(t)$ is a sine wave subcarrier, the power spectral density of the telemetry signal is given by

$$S(f) = P_T[J_0^2(m)\delta(f - f_c) + \sum_{\text{i even}} J_i^2(m)[\delta(f - f_c - if_{sc}) + \delta(f - f_c + if_{sc})] + \sum_{\text{k odd}} J_k^2(m)[S_D(f - f_c - kf_{sc}) + S_D(f - f_c + kf_{sc})]] \quad (10)$$

where $J_k(\cdot)$ is the kth-order Bessel function. The first term in Eq. (10) is the residual carrier spectral component, the second term is the intermodulation loss component, and the third term is the data component.

III. Performance Analysis

On the ground, the carrier component, C(t), of the received signal, s(t), is tracked by the PLL. The tracking performance of the PLL depends on the modulation index m and the tracking loop noise bandwidth-to-data rate ratio (B_L/R_S). Figures l(a) and l(b) illustrate the spectrum of the PCM/PM signals and the portion (shaded area) of the data spectrum that lies within the carrier loop bandwidth B_L. From these figures, it is clear that the interference power is a function of both B_L and R_S. The performance of the carrier tracking loop in the presence of the data is characterized by the interference-to- carrier signal power ratio (ICR). This ratio is determined for all schemes, and the effect of this interference on the phase error process is assessed. Consequently, the SER is calculated for all cases, In order to proceed, a few parameters must be identified. First, the one-sided loop bandwidth of the PLL is defined in terms of the carrier tracking loop transfer function, $H(j2\pi f)$, as follows:

$$B_L = \int_0^\infty |H(j2\pi f)|^2 \, df \tag{11}$$

Current DSN receivers typically use passive second-order PLL filters resulting in [5]

$$|H(f)|^2 = \frac{1 + 2(f/f_n)^2}{1 + (f/f_n)^4} \tag{12}$$

where f_n is the loop natural frequency and is related to the one-sided loop noise bandwidth B_L through

$$B_L = \pi f_n \left(\xi + \frac{1}{4\xi}\right) \tag{13}$$

with ξ denoting the damping factor (typically $\xi = 0.707$ is used). Next, the ICR is determined for the various schemes.

A. Determination of the ICR

From Eq. (1) and Fig. (l), the interference power is that portion of the data spectrum that falls within the carrier loop bandwidth and interferes with the carrier power, as given by Eq. (5). Thus, the ICR becomes

$$ICR = \tan^2(m) \int_0^\infty |H(j2\pi f)|^2 S_D(f) \, df \tag{14}$$

Depending on the data format and rate, Eq. (14) can be simplified further.

1. PCM/PM with ideal NRZ data Format. By substituting Eqs. (7), (12), and (13) into Eq. (14) and evaluating the integral, one obtains

$$ICR = \tan^2(m)\left[\frac{1}{2} + \frac{1}{4\gamma\sqrt{2}}\left(1 - e^{-\gamma\sqrt{2}}\left(\cos(\gamma\sqrt{2}) + 3\sin(\gamma\sqrt{2})\right)\right)\right] \quad (15)$$

where

$$\gamma \triangleq \frac{B_L}{R_S} \quad (16)$$

The upper and lower bound for the ICR can be found from Eq. (15). If one lets **7** approach zero (i.e., the data rate R_S approaches infinity) and by using L'Hospital's rule, one gets the lower bound

$$ICR = 0 \quad (17)$$

On the other hand, if one lets y approach infinity (R_S approaches zero), then one obtains the upper bound

$$ICR \leq \frac{\tan^2(m)}{2} \quad (18)$$

From these bounds, it is clear that as the loop bandwidth-to-data rate ratio, 7, increases, the ICR increases. These results are obvious from Figs. l(a) and (b), because as B_L increases, the shaded area representing the interference due to the data increases while the residual carrier power P_c remains unchanged. Also from Eq. (15), one notices that for a fixed 7, the ICR increases as m increases, since for a fixed total power P_T, PC decreases as m increases (remember $O < m < \pi/2$) while P_D increases. Using Eq. (15), the ICR is plotted in Fig. 2(a) as a function of 7 for different values of m. The appropriate values of γ can be determined for a given modulation index m so that the ICR doea not exceed the maximum allowable value. For a deep space mission, the maximum allowable interference for the carrier tracking is $(ICR)_{max} = -15$ dB, as recommended by the International Radio Consultative Committee (CCIR) [3]. Another important parameter is the critical value of γ (for a given m) that will cause the ICR to reach its maximum allowable value. These critical values for 7 as a function of m are plotted in Fig. 2(b). The region on this graph corresponding to values of y that yield an ICR ratio below the maximum allowable value is called the operating region (OR). From Fig. 2(b), one can see that γ decreases as m increases in order to keep the ICR fixed.

For the NRZ data format case, determining the performance is of interest in the following two special cases. For the high data rate case, the data power spectrum that falls into the carrier tracking loop bandwidth is essentially constant over the tracking loop bandwidth. Thus, for $y < 0.1$, the interference can be considered as additional additive white noise and Eq. (14) can be approximated by

$$ICR \approx \tan^2(m) S_D(0) \int_0^{\infty} |H(f)|^2 \, df \tag{19}$$

or

$$ICR \approx \left(\frac{B_L}{R_S}\right) \tan^2(m) \text{ when } \frac{B_L}{R_S} < 0.1 \tag{20}$$

For the low data rate case, all the power of the interference component falls within the carrier tracking loop bandwidth. Thus, the ICR can be approximated by

$$ICR \approx \tan^2(m) \frac{1}{R_S} \int_0^{\infty} \frac{\sin^2(\pi f/R_S)}{(\pi f/R_S)^2} \, df \tag{21}$$

When $B_L/R_S > 10$, the above integral is easily evaluated:

$$ICR \approx \left(\frac{1}{2}\right) \tan^2(m) \tag{22}$$

In practice, the above case is possible when a data rate of 32 bps is transmitted and a wide carrier tracking mode at $2B_L$ = 300.3 Hz is selected by the ground station receiver.

2. **PCM/PM** With Bi-Phase Data Format. By substituting Eqs. (7) for the hi-phase spectrum and Eq. (12) into Eq. (14) and evaluating the integral, one obtains

$$ICR = \tan^2(m)\left[\frac{1}{2} + \frac{9}{167} - \frac{3}{4\gamma} e^{-2\gamma/3}\left(\cos\left(\frac{2\gamma}{3}\right) + 3\sin\left(\frac{2\gamma}{3}\right)\right)\right.$$

$$\left. + \frac{3}{16\gamma} e^{-4\gamma/3}\left(\cos\left(\frac{4\gamma}{3}\right) + 3\sin\left(\frac{4\gamma}{3}\right)\right)\right] \tag{23}$$

The above ICR is plotted in Fig. 3(a) as a function of γ for various values of m. The corresponding operating region for the ratio γ is plotted in Fig. 3(b).

3. **PCM/PSK/PM.** This scheme is used to separate the residual carrier and the data components so that the interference caused by the data to the residual carrier is minimized. The higher the subcarrier-frequency-to-data rate ratio is, the less the interference. The ICR will be derived for the case of the square wave subcarrier, and the results can be extended to the sine wave case very easily, The data component spectrum can be extracted from the transmitted signal spectrum, aa given by Eq. (9), and is equal to

$$S_{\text{Data}}(f) = \left(\frac{4}{\pi^2}\right) \sum_{k \geq 1} [[S_D(f - (2k-1)f_{sc}) + S_D(f - f_c + (2k-1) f_{sc})]/(2k-1)^2] \quad (24)$$

where $S_D(f)$ is given in Eq. (7), and $f_{sc} = n \times R_s$. By substituting Eqs. (13) and (24) in Eq. (14) and evaluating the integral numerically for the case when $f_{sc} = 3 \times R_s (n = 3)$, one obtains values for the ICR as a function of γ when the modulation index, m, is chosen to have the values 0,9 and 1.3 rad, respectively. The results are plotted in Fig. 4 where it is found that when m = 0.9 rad, the ICR never reaches the maximum allowable value when $\gamma \leq 1$. However, a critical value of $(\gamma)_{CR}$ = 0.56 is found when the modulation index is increased to m = 1.3 rad. In Fig. 4(a), it is shown that the ICR decreases rapidly for the two modulation indices when $\gamma < 0.2$. The above procedure was repeated for $n \geq 3$ and it was found that the interference is negligible. Note that for the PCM/PSK/PM scheme, the critical value for γ is quite large even at the largest modulation index chosen, m = 1.3 rad. The same cannot be said about the PCM/PM scheme where one must operate at values of y much below 1, in order to keep the ICR below – 15 dB,

B. The Effect of the Interference on Carrier Tracking Phase Error

When the received signal is tracked by a PLL, the phase error process, defined aa

$$\phi(t) = e(t) - e(t) \quad (25)$$

haa contributions from both the thermal noise and the interference caused by the data. The accuracy of the estimate $\hat{\theta}(t)$ is dependent on the power allocated to the residual carrier component. Under the high data rate assumption, the data interference component has a spectrum over the PLL bandwidth, and hence it can be considered aa an additional additive white noise. In this case, the variance of the phase error due to the combined additive Gaussian noise is given by [6]

$$\sigma^2 = \frac{N B_L}{P_c} \quad (26)$$

where N is the effective noise spectral density resulting from thermal noise and data interference, and is determined as follows:

$$N = \frac{1}{B_L} \int_0^\infty |H(j2\pi f)|^2 [N_0 + P_D S_D(f)] \, df \quad (27)$$

Alternatively, one has

$$N = N_0 + \frac{P_D}{B_L}\alpha \tag{28}$$

where

$$\alpha \triangleq \int_0^\infty S_D(f)|H(j2\pi f)|^2\, df \tag{29}$$

Rather than expressing the variance of the phase error in terms of the modified noise spectral density N, it will be expressed in terms of the ICR to show the interdependence explicitly. Thus, under the high data rate assumption, the variance of the carrier tracking phase error becomes [7]

$$\sigma^2 = \frac{1}{P} = \frac{1}{\rho_0} + ICR \tag{30}$$

where p is the effective loop SNR, and ρ_0 is the carrier loop signal-to-thermal-noise power ratio defined as

$$\rho_0 = \frac{P_C}{N_0 B_L} = \frac{Es/N.}{(B_L/R_S) \times \tan^2(m)} \tag{31}$$

Under the linear operation assumption, the probability density function (pdf) of the phase error process may be approximated by the Tikhonov pdf [1). Hence the pdf of $\phi(t)$ is completely determined, once p is known, from

$$p(\phi) \cdot \frac{\exp(\rho\cos\phi)}{2\pi I_0(\rho)} \text{ when } -\pi \leq \phi \leq \pi \tag{32}$$

where $I_0(\cdot)$ is the modified Bessel function of the first kind, and p is the effective loop SNR, which is the inverse of the variance σ^2 of the carrier tracking phase error. Now, this variance for all cases must be found.

1. PCM/PM With Ideal NRZ Data Format. For the NRZ data format, the performance will be determined for the low-data-rate case as well as the high-data-rate case.

a. ***High-Data- Rate Case*** $(B_L/R_S < 0.1)$, The expression for the ICR for this case is found in Eq. (20), which when substituted in Eq. (30), gives the phase error variance

$$\sigma^2 = \frac{1}{\rho} = \frac{1}{\rho_0} + \left(\frac{B_L}{R_S}\right)\tan^2(m) \tag{33}$$

The inverse of the phase error variance, i.e., the effective loop SNR as a function of symbol SNR (SSNR) is plotted in Figs, 5(a) and 5(b) for this case. The region corresponding to values of $\rho < 8$ dB is called the PLL nonoperating region (PLLNOR). This is the region where the loop is slipping cycles and should be avoided.

b. Very Low-Da ta-Rate Case ($B_L/R_S > 10$). Here one cannot treat the data interference as just additional white noise, but rather the procedure chosen by Youn and Lindsey [8] will be followed. When the data rate is very low, the carrier interference component, $I_C(t)$, can be treated as a CW interference with its phase switching slowly and randomly between O and π with respect to the phase of the residual carrier. Thus, if one lets $\Delta\theta$ be the phase difference between the interference component $I_C(t)$ and the carrier component C(t), then within the tracking loop bandwidth, $\Delta\theta$ will take on the values O and π with equal probability. The Fokker–Plank method can be used to derive the pdf for the carrier tracking phase error, Let ϕ denote the carrier tracking phase error induced by $I_C(t)$ and the AWGN, $n(t)$. 'l'hen the conditional pdf, $p(\phi|\Delta\theta)$, in the presence of CW interference can be approximated as

$$P_W(\phi|\Delta\theta) \cong \left| \frac{\exp\left[-(\phi - M)^2/2\sigma^2\right]}{\sqrt{2\pi\sigma^2}\ \mathrm{erf}\left(\pi/\sqrt{2\sigma^2}\right)} \right|_{\text{I'or}} \quad |\phi| \leq \pi \tag{34}$$

where M and σ^2 are the conditional mean and variance of the phase error ϕ, respectively, and they are defined as

$$M = -\frac{\sqrt{ICR}\ \sin(\Delta\theta)}{1 + \left(\sqrt{ICR}\ \cos(\Delta\theta)\right)} \tag{35}$$

$$\sigma^2 = \frac{1}{\rho_0\left[1 + \sqrt{ICR}\ \cos(\Delta\theta)\right)} \tag{36}$$

By using Bayes' rule, the conditioning on $\Delta\theta$ can be removed to obtain the pdf of the phase error process:

$$p(\phi) = \frac{1}{2}\left[\frac{\exp[-\phi^2/2\sigma_+^2]}{\sqrt{2\pi\sigma_+^2}\ \mathrm{erf}(\pi/\sqrt{2\sigma_+^2})} + \frac{\exp[-\phi^2/2\sigma_-^2]}{\sqrt{2\pi\sigma_-^2}\ \mathrm{erf}(\pi/\sqrt{2\sigma_-^2})}\right] \tag{37}$$

where

$$U^2 = \frac{1}{\rho_0\left(1 \pm \sqrt{ICR}\right)} \tag{38}$$

The above approximation is valid only when the ICR < 1, which is the case of interest here. The effective loop SN R is depicted in Fig. (6) as a function of the SSNR when γ = 10. The above pdf will be used to derive the SER for the low data rate case instead of the Tikhonov pdf that is used in the high data rate case.

2. **PCM/PM** With Ideal **Bi-Phase** Data Format. Under the high data rate assumption, the variance of the phase error process is given earlier in Eq. (30). By substituting the expression for the ICR derived in Eq. (23), the variance is determined, and consequently the Tikhonov pdf is now completely characterized. As mentioned before, in order to specify the PLL operating region, the inverse of the phase error variance is plotted as a function of SSNR in Figs. 7(a) and 7(b) for different modulation indices.

3. **PCM/PSK/PM.** By substituting the numerical values for the ICR obtained in Section (III.A.3) when m = 1.3 rad and the ratio $B_L/R_S = 0.05$ in Eq. (30), one obtains the phase error variance for the square-wave sub carrier. The RMS of this variance is plotted as a function of loop SNR, ρ_0, in Fig. 8 for n = 1 and n = 3 where n is the subcarrier frequency to bit rate, as defined earlier. The figure indicates that if one chooses the integer $n \geq 3$, then the performance of this scheme is almost identical to that of the ideal case. The ideal case refers to the binary phase-shift keying (BPSK) modulation scheme over an AWGN channel.

C. Effect of Interference on the SER Performance

The symbol error probability for uncoded PSK transmission over a Gaussian channel disturbed by additive white noise of one-sided spectral thermal noise density N_0 is given by [1, Chap. 5]

$$P_S = \frac{1}{2}\,\mathrm{erfc}\left(\sqrt{\frac{E_S}{N_0}}\right) \tag{39}$$

The conditional symbol error probability that takes into account the phase error process is given by [6]

$$P_S(\phi) = \frac{1}{2}\,\mathrm{erfc}\left(\sqrt{\frac{E_S}{N_0}}\,Y(\phi)\right) \tag{40}$$

where

$$Y(\phi) = \frac{1}{T_S}\int_0^{T_S} \cos[\phi(t)]\,dt \tag{41}$$

Then the unconditional symbol error probability can be obtained by averaging $P_S(\phi)$ over ϕ, i.e.,

$$P_S = \int_{-\pi}^{\pi} P_S(\phi)\ p(\phi)d\phi \tag{42}$$

1. PCM/PM With Ideal NRZ Data Format

a. High-Data-Rote Case. When the data rate is high with respect to the receiver tracking loop bandwidth (i.e., $\gamma <$ 0.1), the phase error process $\phi(t)$ varies slowly and is essentially constant over a symbol interval ***Ts.*** Then from Eq. (41), it is concluded that for this case

$$Y(\phi) \approx \cos\phi \tag{43}$$

and the average symbol error probability is obtained by substituting Eq. (43) in Eq. (42) to give

$$P_S = \frac{1}{2}\int_{-\pi}^{\pi} \operatorname{erfc}\left(\sqrt{\frac{E_S}{N_0}}\ \cos\phi\right)\ \frac{\exp(\rho\cos\phi)}{2\pi I_0(\rho)}d\phi \tag{44}$$

This SER, P_S, *is* plotted in Fig. 9(a) **as** a function of SSNR ***(Es/No)*** for different values of m when γ = 0.005. From this figure, one sees that when m = 1.3 rad, the degradation becomes considerable. Figure 9(b) depicts that even when ***m*** = 1.3 rad, the performance can be improved by decreasing γ, i.e., by either increasing the data rate or by decreasing the loop noise bandwidth. For Figs. 9(a) and 9(b) to be useful, they must be used in the operating region of the PLL, **as** given earlier in Figs. 5(a) and 5(b). For example, when γ = 0.01 and m = 1.3 rad, Fig. 5(b) indicates that the **PLL** locks, provided that the SSNR **is** at leaat 8 dB. Therefore, when using the performance curve corresponding to the above operating conditions [Fig. 9(b)], only the region where the SSN R $\geq$ 8 dB ia useful.

b. Vey Low-Data-Rate Case. When the data rate is low relative to the receiver tracking loop bandwidth, the phase process $\phi(t)$ varies rapidly over the symbol interval ***Ts.*** Hence, the random variable $Y(\phi)$, as given in Eq. (41), is a good approximation of the true time average of the function $\cos[\phi(t)]$. When $\phi(t)$ can be modeled **as** an ergodic process, the time average may be replaced by the statistical mean. **Thus,**

$$Y(\phi) \simeq E\{\cos\phi\} = \int_{-\pi}^{\pi} \cos\phi \times p(\phi)d\phi = C_0 \tag{45}$$

The constant C_0 can be computed by substituting the expression for the **pdf** of the phase error derived from **Eq.** (37) in **Eq.** (45). Then, by substituting in **Eqs.** (41) and (43) one obtains the average symbol error probability

$$P_S = \frac{1}{2}\,\mathrm{erfc}\left(\sqrt{\frac{E_S}{N_0}}\,C_0\right) \tag{46}$$

In Fig. 10, P_S is plotted as a function of SSNR for different values of m when γ = 10. The figure shows that the degradation is substantial and becomes worse as m increases. It should be noted that the approximation used is valid when $ICR < 1$, which corresponds to $m \leq 0.955$ rad. However, Fig. 6 indicates that in order for the PLL to maintain lock, one must operate at an SSNR higher than 20 dB, even for the smallest modulation index chosen (0.7 rad), an impractical requirement to say the least. Therefore, the PCM/PM modulation technique with the NRZ data format is not a viable choice when $B_L \geq$ Rs.

2. **PCM/PM With Bi-Phase Data Format.** Assuming that the data rate is high, i.e., 7 < 0.1, the random variable $Y(\phi)$ is approximated aa in Eq. (43). By substituting the result and the appropriate Tikhonov pdf for this case, aa derived in Eq. (42), one obtains an expression for the SER. This average SER is calculated aa a function of the SSNR E_S/N_0 for different values of m when γ = 0.05, and the results are plotted in Fig. 1 l(a). One sees that a noticeable degradation is observed only for the case when m = 1.3 rad. The effect of varying γ is shown in Fig. n(b) for m = 1,3 rad. When 7 = 0.005, the performance of the loop SNR approaches that of the ideal case.

3. **PCM/PSK/PM.** By substituting the calculated phase error variance obtained in Section III, B.3 and Eq. (42), it is found that when the integer n $\geq$ 3, the performance approaches that of the ideal case. Whereas when n = 1, the performance is identical to the PCM/PM scheme with the bi-phaae data format case, aa it should be

IV. Discussion and Summary of the Results

A. Theoretical Results

The critical values of 7 for a given modulation index for which the ICR exceeds the CCIR recommended threshold value of – 15 dB are obtained. These values are given in Table 1 for all the schemes when m = 0.9 and 1.3 rad.

From Table 1, one notes that for a given modulation index, the PCM/PM scheme with the NRZ data format requires a value of 7 smaller than the other two schemes to operate at the threshold interference level. The PCM/PSK/PM scheme performs just aa well at a much larger 7 ratio when n = 3 or higher.

The SER and the effective loop SNR of the PCM/PM scheme with both NRZ and hi-phase data formats, as well as the ideal case, are superimposed in Figs. 12(a) and 12(b) when m = 1.3 rad for different values of 7, in order to compare

their performance, The criterion is the degradation in SSNR for the particular scheme considered relative to the ideal case, i.e., the required increase in SSNR in order to achieve the same performance as the ideal case. This degradation is due to both the thermal noise and the data interference. The SSNR degradation of the three schemes considered is obtained for different values of m and γ from the figures and is summarized in Tables 2–5.

In Table 2, the chosen value for γ is very small and is below the critical value (see Table 1) for all the schemes. One notes a very small degradation for the PCM/PM/NRZ scheme and negligible degradation for the other two schemes. Table 3 shows the effects of increasing 7.

In Table 4, the dependence of the performance on the modulation index is demonstrated. The loop bandwidth-to-data rate ratio is unchanged from the previous table, but the modulation index is smaller. It is observed that the performance of the PCM/PM/NRZ scheme improves as the modulation index decreases.

In Table 5, both PCM/PM schemes are in the not-recommended region (NRR) (see Table 1). The two PCM/PM schemes can be compared in terms of the effective loop SNR for the same values of SSNR, m and γ. The scheme with the higher effective loop SNR performs better, Using Figs. 5(b) and 7(b), the values are tabulated in Table 6. It is observed that for the same operating parameters, the PCM/PM/bi-phase scheme always has a higher effective loop SNR than the PCM/PM/NRZ scheme.

The unfiltered occupied bandwidth with 99-percent power containment as a function of the modulation index for both PCM/PSK/PM and PCM/PM signals was derived in [9]. The results are summarized here in Fig. 13. As expected, it is shown that the PCM/PM scheme with the NRZ data format requires the least occupied bandwidth and the PCM/PSK/PM scheme requires the most. The bandwidth occupancy increases linearly with the modulation index for all the schemes.

B. Measured Performance

The measured SER values for all schemes *were* obtained by using the Advanced Receiver (ARX) 11. A functional description of the ARX 11 is presented in [10]. Figures 14(a), 14(b) and 14(c) depict the measured performance for the PCM/PM/NRZ signal when the ICR = –24 dB, – 18.6 dB and –15.8 dB. It is clear that the model predicts the measurements for ICR < – 15 dB. As the ICR increases, the measurements diverge from the model, as shown in Fig. 14(c). The same observations are reported for the PCM/PM/bi-phase signal type, as evident in Figs. 15(a), 15(b), and 15(c). However, for this signal type the deviation of the measured values from the theoretical values is less than that

of the NRZ signal type for the same m and 7. The above deviations indicate that the assumptions made by regarding the data interference as additional white noise are valid as long as 7 is less than a threshold value, as specified in Table 1. Figure 16 indicates that for the PCM/PSK/PM case, the measured performance is identical to the theoretical performance when $m = 1.1$ rad and $\gamma = 0{,}001$.

V. Conclusion

In this paper, the performance of the PCM/PM/NRZ scheme was considered in the limiting two cases of high and very low data rates and the performance of PCM/PM/bi-phase scheme was considered for the high-data-rate case and compared with the PCM/PSK/PM scheme. As long as the PLL implementation by the DSN is used, the following conclusions are valid. In terms of SER performance, the PCM/PSK/PM scheme is better than the PCM/PM scheme (both NRZ and bi-phase) when the loop bandwidth-to-data rate ratio is not small enough, as discussed in the previous section. However, the PCM/PSK/PM scheme requires a great deal of bandwidth. In terms of bandwidth efficiency, the PCM/PM/NRZ scheme is the best but has higher degradation for $7 \geq 0.001$ and $m = 1.3$ rad. As a compromise, the PCM/PM/bi-phase scheme can be used with twice the bandwidth of the PCM/PM/NRZ scheme but with much less degradation. However, at a very small loop bandwidth-to-data rate ratio, which at present the DSN receivers are capable of supporting, the performance of the PCM/PM schemes coincides with that of the PCM/PSK/PM scheme. In addition, if one takes into account the sub carrier loss in the receiver when the PCM/PSK/PM scheme is employed, the performance of PCM/PM schemes becomes as good if not better than that of the PCM/PSK/PM scheme. Moreover, under these conditions the PCM/PM/NRZ scheme becomes the most attractive because it requires the least of bandwidth occupancy. If PLL-based receiver implementation is not required, then the BPSK scheme without a residual carrier is most attractive.

Acknowledgments

The authors thank Dr. V. Vilnrotter for all of his valuable comments and Brenda Goforth for her help in preparing this article for submission.

References

[1] J. Yuen, Ed., ***Deep Space Telecommunications Systems Engineering, New*** York: Plenum Press, 1983.

[2] Consultative Committee for Space Data Systems, ***Recommendations for Space Data System Standards, Radio Frequency and Modulation Systems, Part 1, Earth Stations and Spacecraft,*** CCSDS 401.0-B, Blue Book, Washington, DC: NASA, CCSDS Secretariat, Communications and Data Systems Division (Code OS), 1989.

[3] International Radio Consultative Committee (CCIR), ***Recommendations and Reports of the CCIR, XVIth Plenary Assembly, Volume II: Space Research and Radio Astronomy,*** "Protection Criteria and Sharing Considerations Relating to Deep Space Research," Rep. 685-2, Dubrovnik, pp. 278-289, 1986.

[4] J. K. Holmes, ***Coherent Spread Spectrum Systems, New*** York: John Wiley and Sons, 1982,

[5] T. M. Nguyen, "Closed Form Expressions for Computing the Occupied Bandwidth of PCM/PSK/PM Signals," ***Proceedings of the IEEE International Symposium on EMC,*** Cherry Hills, New Jersey, August 1991,

[6] W. C. Lindsey and M. K. Simon, ***Telecommunications Systems Engineering,*** Englewood Cliffs, New Jersey: Prentice-Hall, 1973.

[7] T. M. Nguyen, "Space Telemetry Degradation Due to Manchester Data Asymmetry Induced Carrier hacking Phase Error," ***IEEE Transactions on EMC, vol. 33,*** no. 3, pp. 262–268, August 1991.

[8] C. Y. Youn and W. C. Lindsey, "Phase-Locked Loop Performance in the Presence of CW Interference and Additive Noise," ***IEEE Transactions on Communications,*** vol. COM-30, no. 10, pp. 2305-2311, October 1982.

[9] T. M. Nguyen, "Occupied Bandwidths for PCM/PSK/PM and PCM/PM Signals-A Comparative Study," CCSDS Subpanel 1E, RF and Modulation Meeting, Salzburg, Austria, May 1992.

[10] S. M. Hinedi, "NASA's Next Generation Deep Space Network Breadboard Receiver," to be published in Jan 93 issue of ***IEEE Transactions on*** Communications.

Table 1. Critical values of $(\gamma)_{CR}$.

Modulation index, red	γ		
	PCM/PM/NRZ	PCM/PM/bi-phase	PCM/PSK/PM, $n = 3$
0.9	0.010	0.235	**Any value**
1.3	**0.002**	0.03s	**0.56**

Table 2. **SSNR degradation when** $\gamma = 0.001$ **●** nd $m = 1.3$ **rad.**

SER	SSNR degradation. dB		
	PCM/PM/NRZ	PCM/PM/bi-phase	PCM/PSK/PM, $n = 3$
10^{-3}	*0.04*	Negligible	Negligible
10-'	**0.06**	Negligible	Negligible
10-'	**0.09**	**Negligible**	**Negligible**

Table 3. **SSNR degradation** when $\gamma = 0.00S$ and $m = 1.3$ **rad.**

SER	SSNR degradation, dB		
	PCM/PM/NRZ, NRR[a]	PCM/PM/bi-phase	PCM/PSK/PM, $n = 3$
10^{-3}	*0.s*	**Negligible**	Negligible
10-'	**0.7**	**Negligible**	**Negligible**
10^{-5}	**1.2**	Negligible	**Negligible**

• **NRR in the column corresponding to the P CM /P M /N RZ scheme refers** to nob **recommendad** region. because **the chosen value for** γ **is greater than the critical value for this** scheme (**see** Table 1). **Therefore, serious** degradation for **that** particular scheme **is observed.**

Table 4. SSNR degradation when $\gamma = 0.005$ and $m = 1.1$ rad.

SER	SSNR degradation, dB		
	PCM/PM/NRZ, NRR[a]	PCM/PM/bi-phase	PCM/PSK/PM, $n = 3$
10^{-3}	0.10	Negligible	Negligible
10^{-4}	0.1s	Negligible	Negligible
10^{-5}	0.20	Negligible	Negligible

[a] NRR = not recommended region.

Table 5. SSNR degradation when $\gamma = 0.0S$ and $m = 1.3$ rad.

SER	SSNR degradation, dB		
	PCM/PM/NRZ	PCM/PM/bi-phase	PCM/PSK/PM, $n = 3$
10^{-3}	NRR[a] PLLNOR[b]	1.2 (NRR)	Negligible
10-4	NRR PLLNOR	1.1 (NRR)	Negligible
10^{-5}	NRR PLLNOR	1.05 (NRR)	Negligible

[a] NRR . not recommended region.
[b] PLLNOR = PLL nonoperating region ($\rho < 8$ dB).

Table 6. **Effective loop SNR when $m = 1.3$ rad and SSNR = 7 dB.**

γ	Effective 100P SNR, ρ, dB	
	PCM/PM/NRZ	PCM/PM/bi-phase
0.050	1.0 (NRR[a], PLLNOR[b])	9.0 (NRR)
0.010	8.0 (NRR),	16.0
0.005	11.5 (NRR)	19.0
0.001	18.0	25.9

[a] NRR = not recommended region.
[b] PLLNOR = PLL nonoperating region ($\rho < 8$ dB).

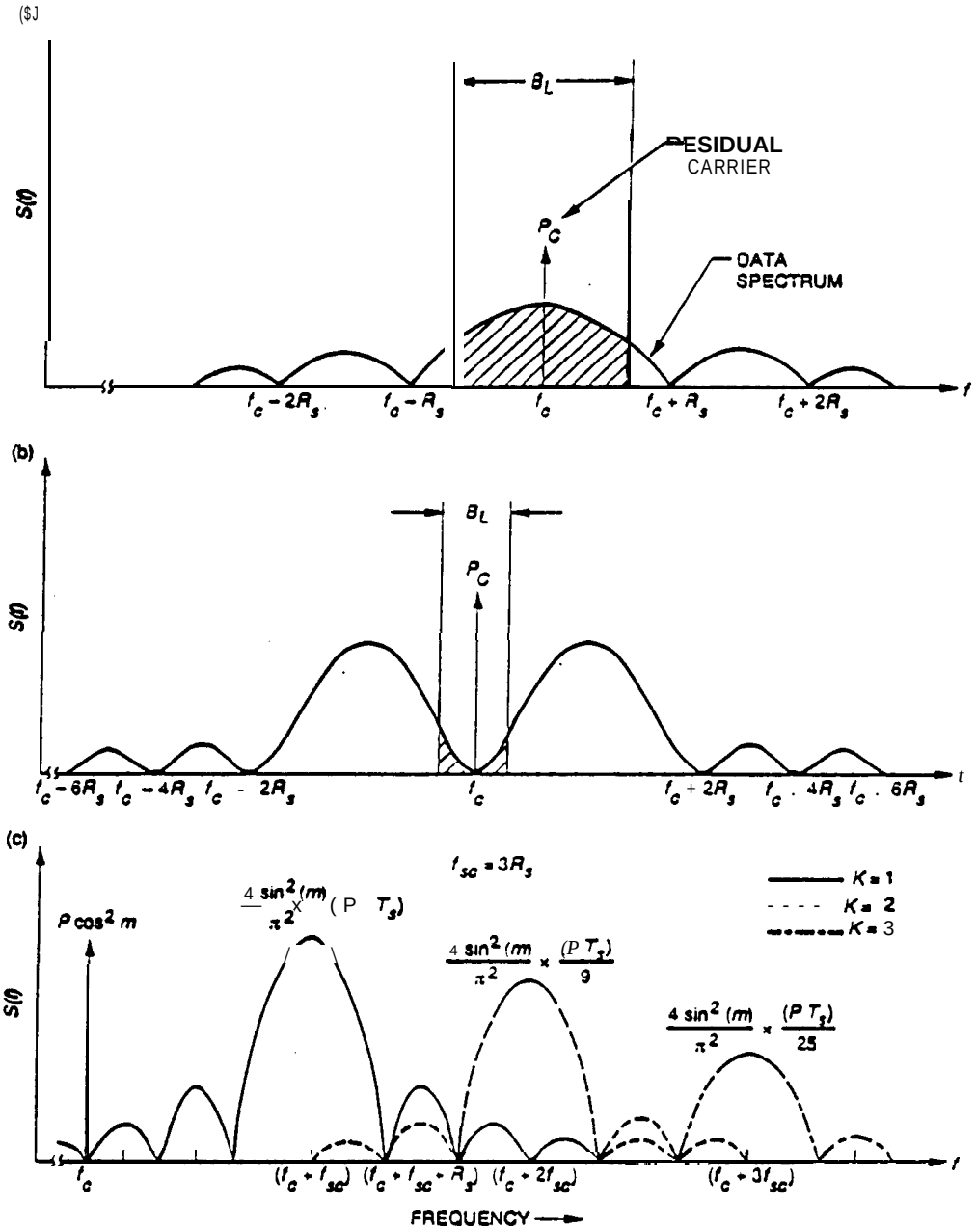

Fig. 1. Interaction between the residual carrier and **the** dote **spectrum:** (a) **Interaction between the residual carrier** ● nd **the** NRZ **data** spectrum when $B_L < R_S$; (b) **Interaction between the residual carrier** snd **the bi-phase data** spectrum **when** $B_L < R_S$; **and** (c) power **spectrum of the residual** carrier with **square waveform as** its **subcarrier.**

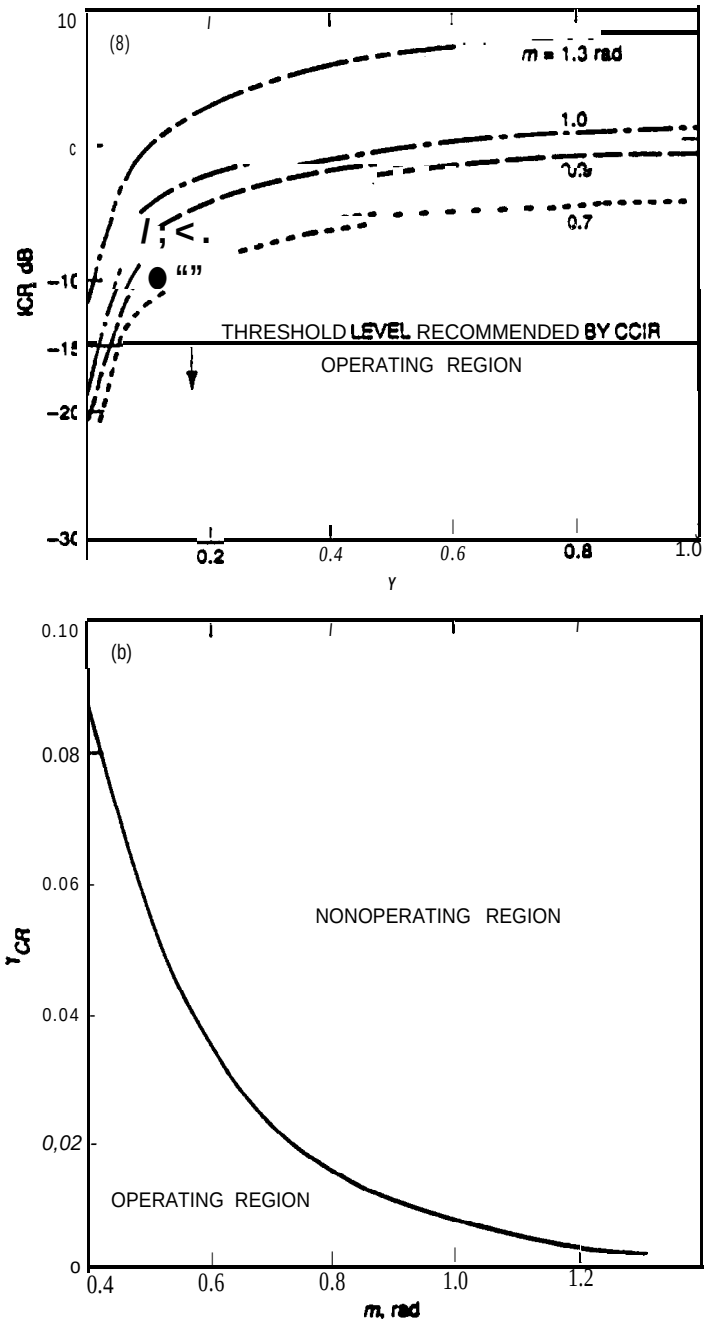

Fig. 2. Effects of the interference duo to the NRZ data format: (a) ICR versus γ tor the PCM/PM/NRZ scheme and (b) γ versus modulation index m when ICR = threshold value of -1S dB for the PCM/PM/NRZ case.

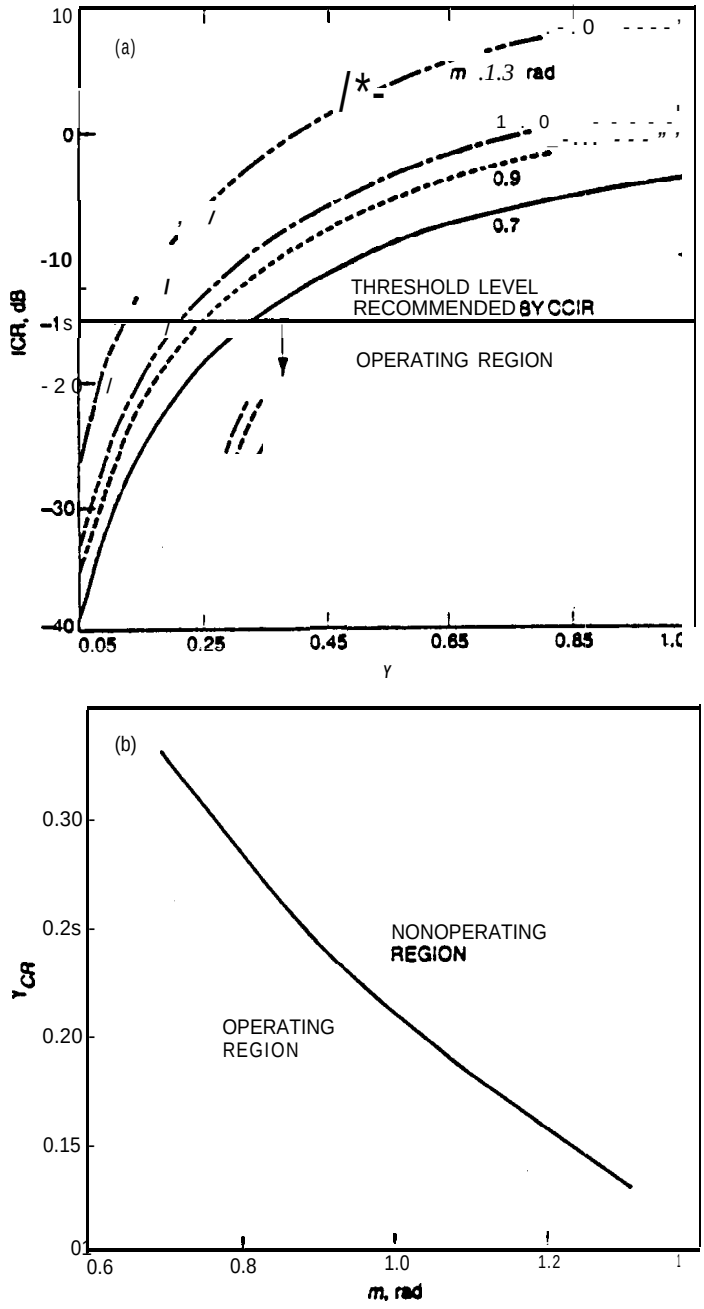

Fig. 3. Effects of the interference duo to the bi-phase data format: (a) ICR versus γ tor PCM/PM/bi-phase ● ohomo ● nd (b) γ versus modulation index m when ICR = −15 dB tor the PCM/PM/bi-phase case.

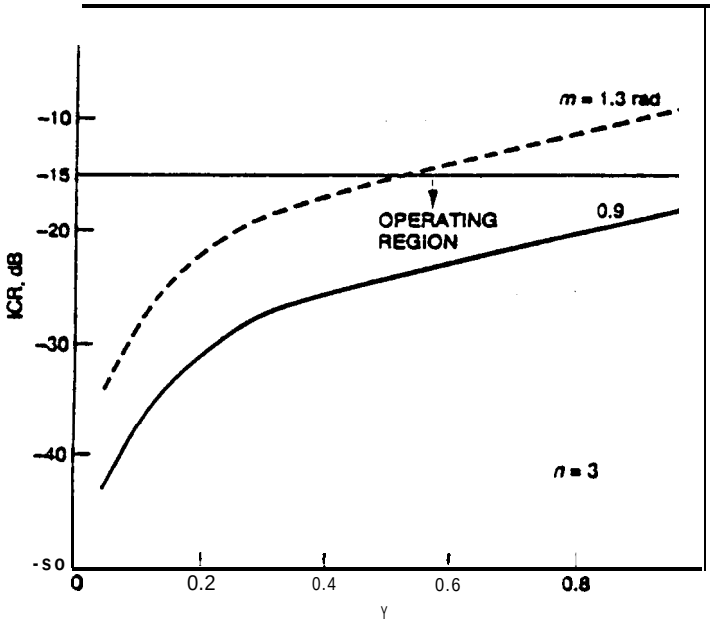

Fig. 4. ICR versus γ for the PCM/PSK/PM scheme with square-wave subcarrier.

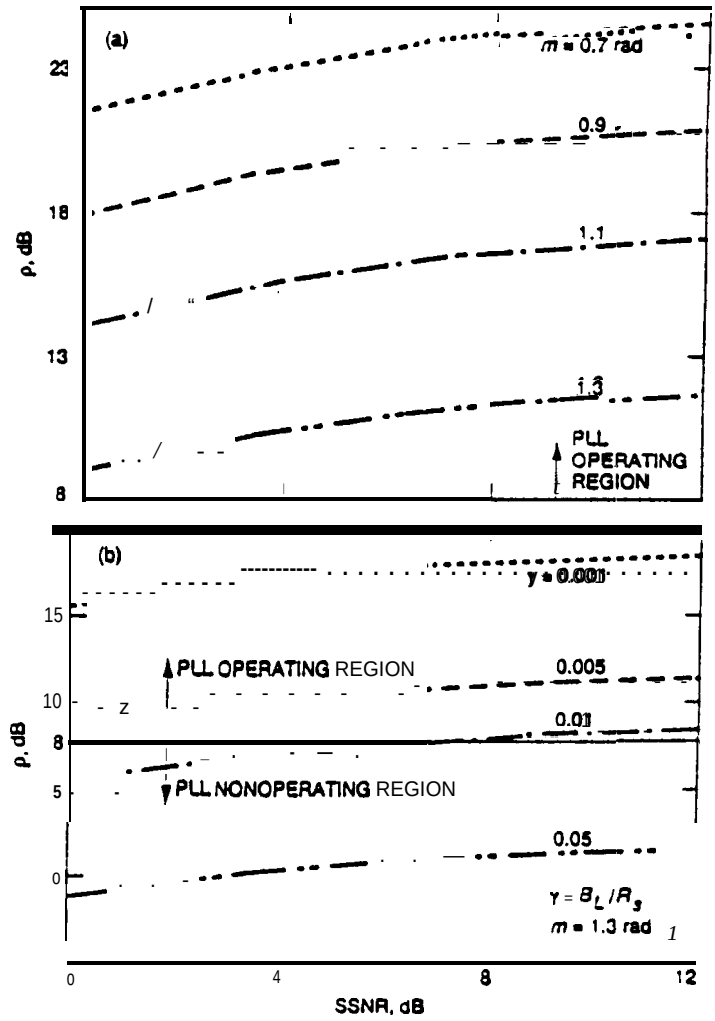

Fig. 5. Effective loop SNR as a function of SSNR and m for PCM/PM/NRZ: (a) ● flootlvo loop SNR versus SSNR for PCM/PM/NRZ (γ = 0.005) and *(b)* ● *tfootivo* loop SNR versus symbol SNR for PCM/PM/NRZ (m=1.3 red).

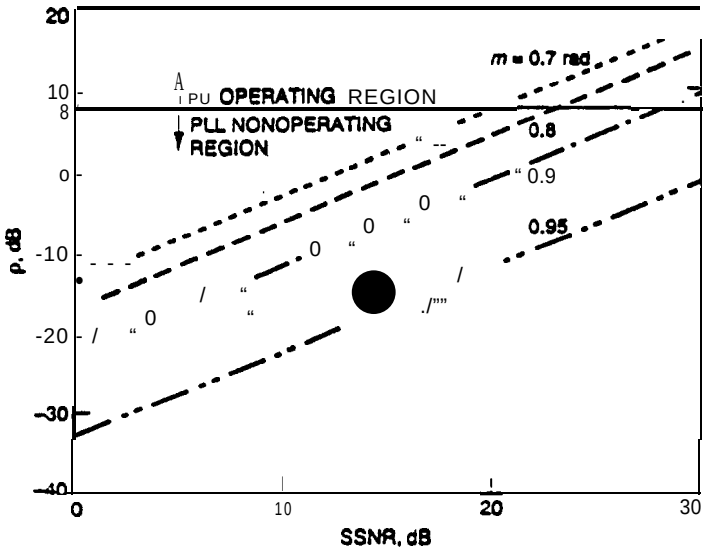

Fig. 6. **Effective loop** SNR **versus SSNR for PCM/PM/NRZ (7 = 10), low data rate case.**

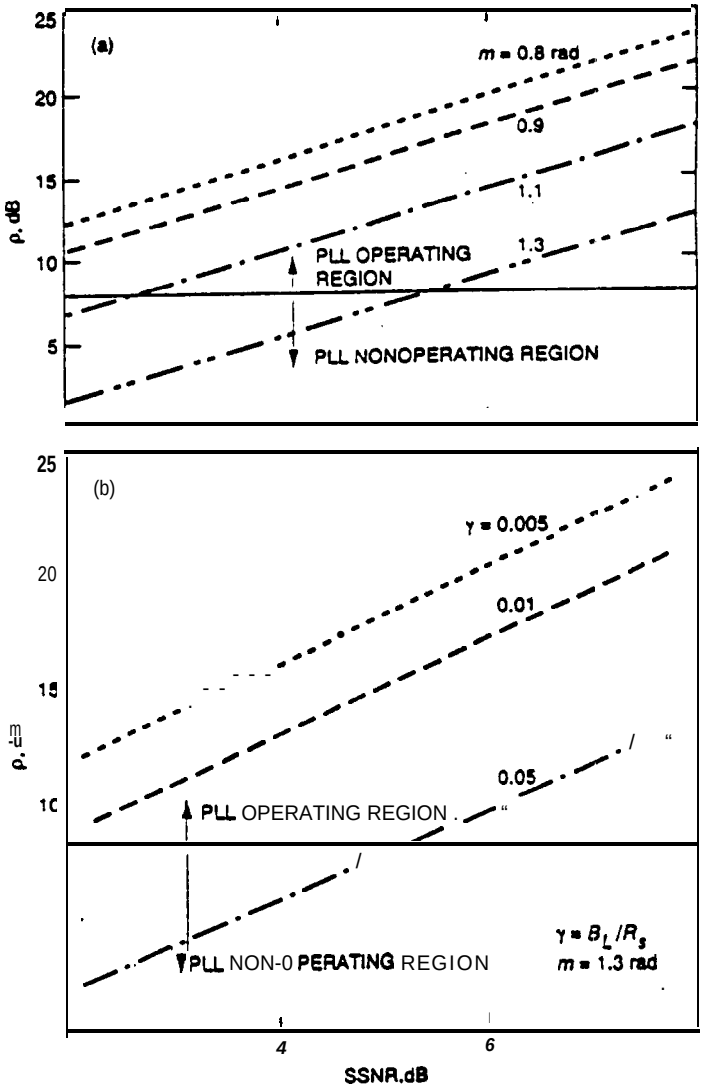

Fig 7. **Effective** loop **SNR** ● **s** ● **function of SNR for PCM/PM/bi-phase: (a)** ● ttoolivo **loop SNR versus SSNR for PCM/PM/bi-phase** (γ = 0.0S) ● nd (b) **effective loop SNR versus SSNR for PCM/PM/bi-phase (*m* = 1.3 rad).**

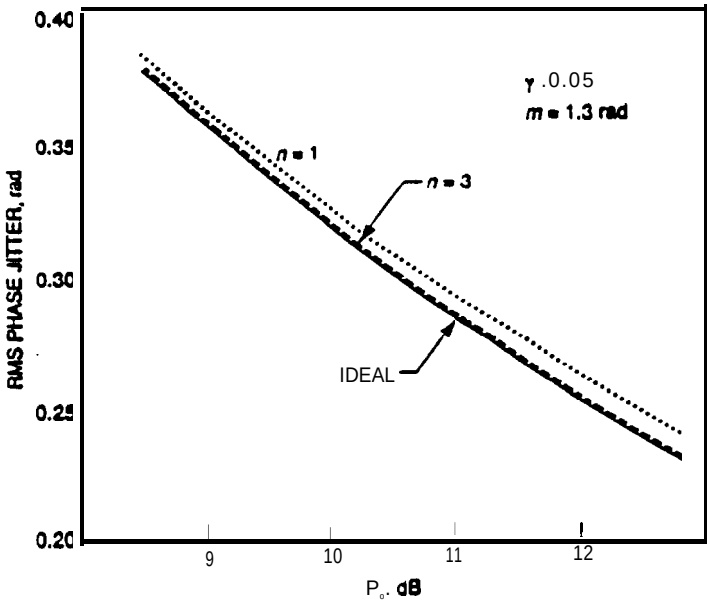

Pig. 8. RMS of phase jitter for the PCM/PM/PSK square-wave case.

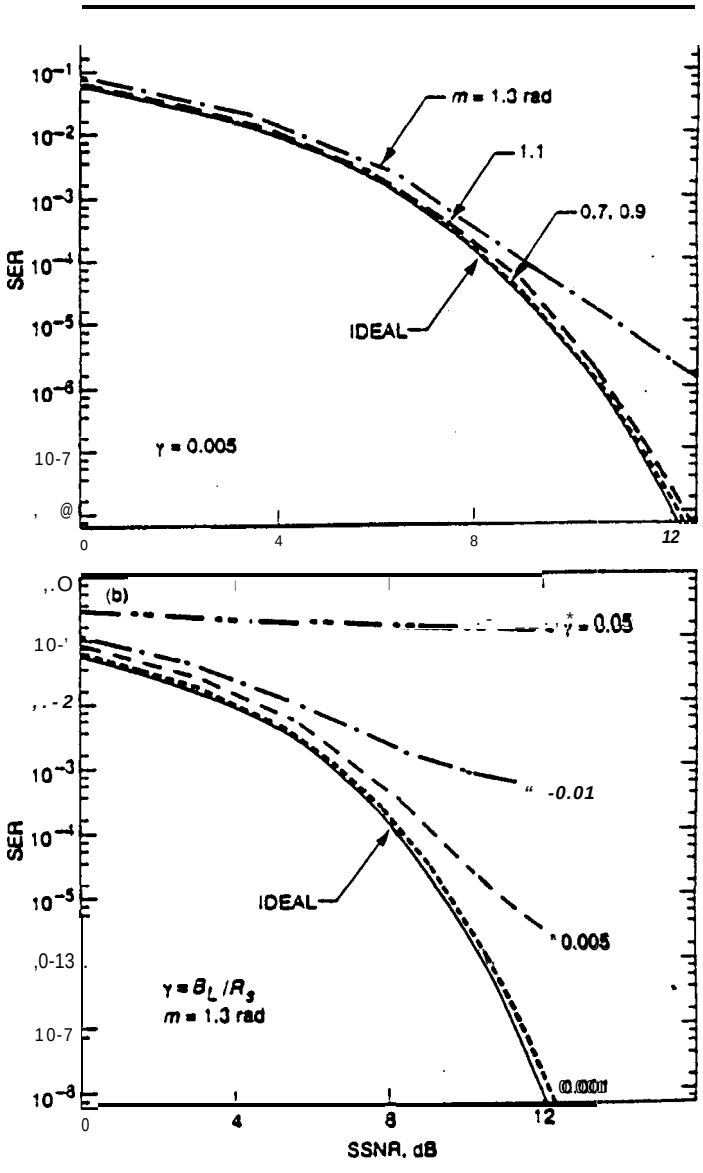

Fig. 9. SER for PCM/PM/NRZ: (a) SER versus SSNR for PCM/PM/NRZ ($\gamma = 0.005$) and (b) SER versus SSNR for PCM/PM/NRZ (m = 1.3 rad).

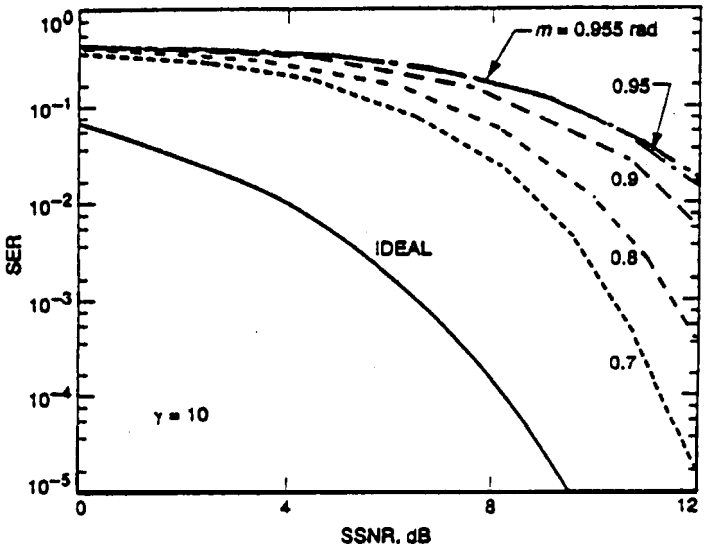

Fig. 10. SER versus SSNR for PCM/PM/NRZ ($\gamma = 10$), low-data rate case.

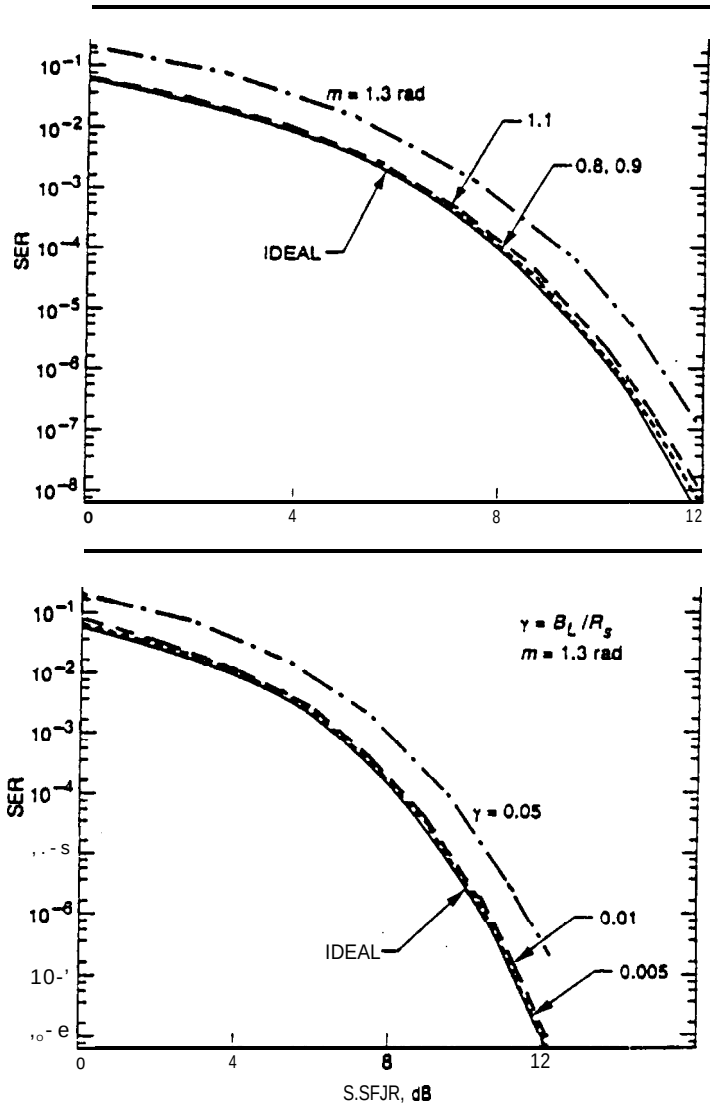

Fig. 11. SER for PCM/PM/bi-phase: (a) SER versus SSNR for PCM/PM/bi-phase (7 = 0.0S) and (b) SER versus SSNR for PCM/PM/bi-phase (m = 1.3 red).

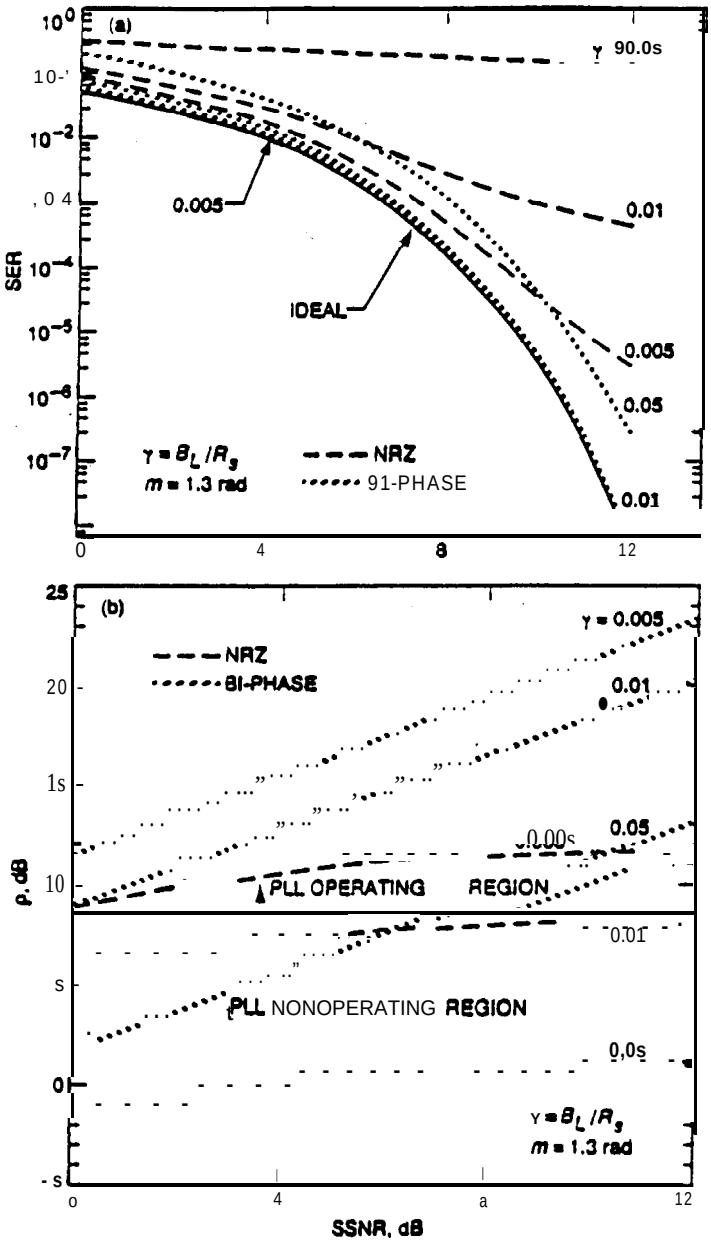

Fig. 12. Performance composition of PCM/PM/NRZ ● nd PCM/PM/ bi-phase: (a) SER versus SSNR for PCM/PM when m = 1.3 rad ● nd (b) effective loop SNR versus SSNR for PCM/PM when *m* = 1.3 rad.

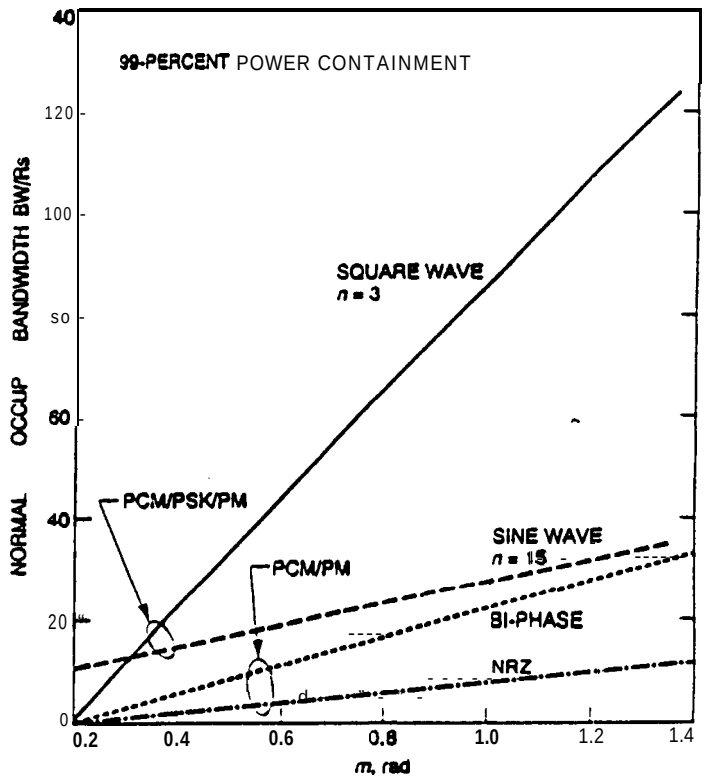

Fig. 13. Bandwidth occupancy of PCM/PSK/PM versus PCM/PM signals.

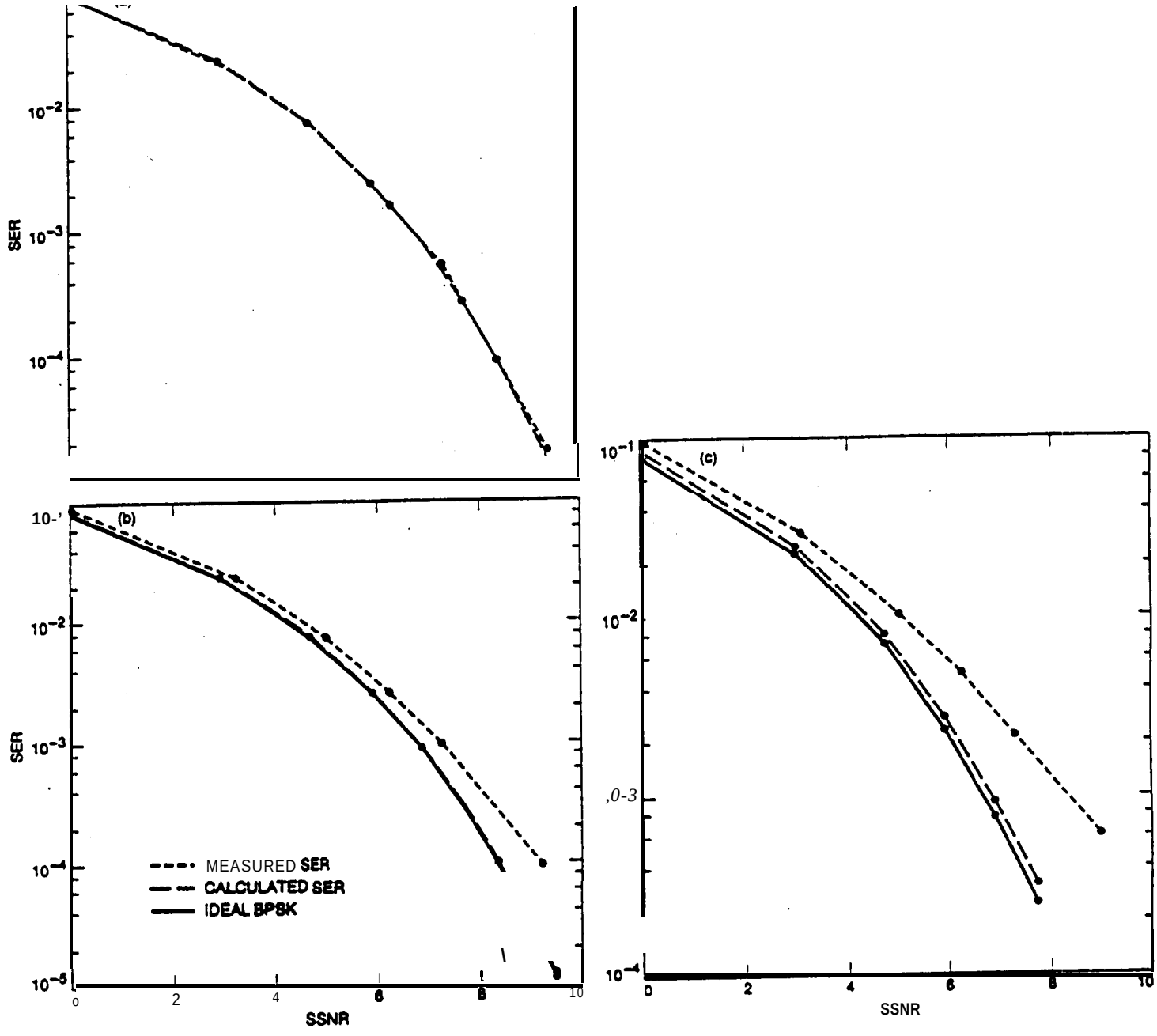

Fig. 14. Measured performance for PCM/PM/NRZ: (a) ICR = -24 dB (m = 1.1 rad, γ = 0.001); (b) ICR = -18.6 dB (m = 1.1 rad, γ = 0.001); and (c) ICR = −15.8 dB (m = 1.3 rad, γ = 0.002).

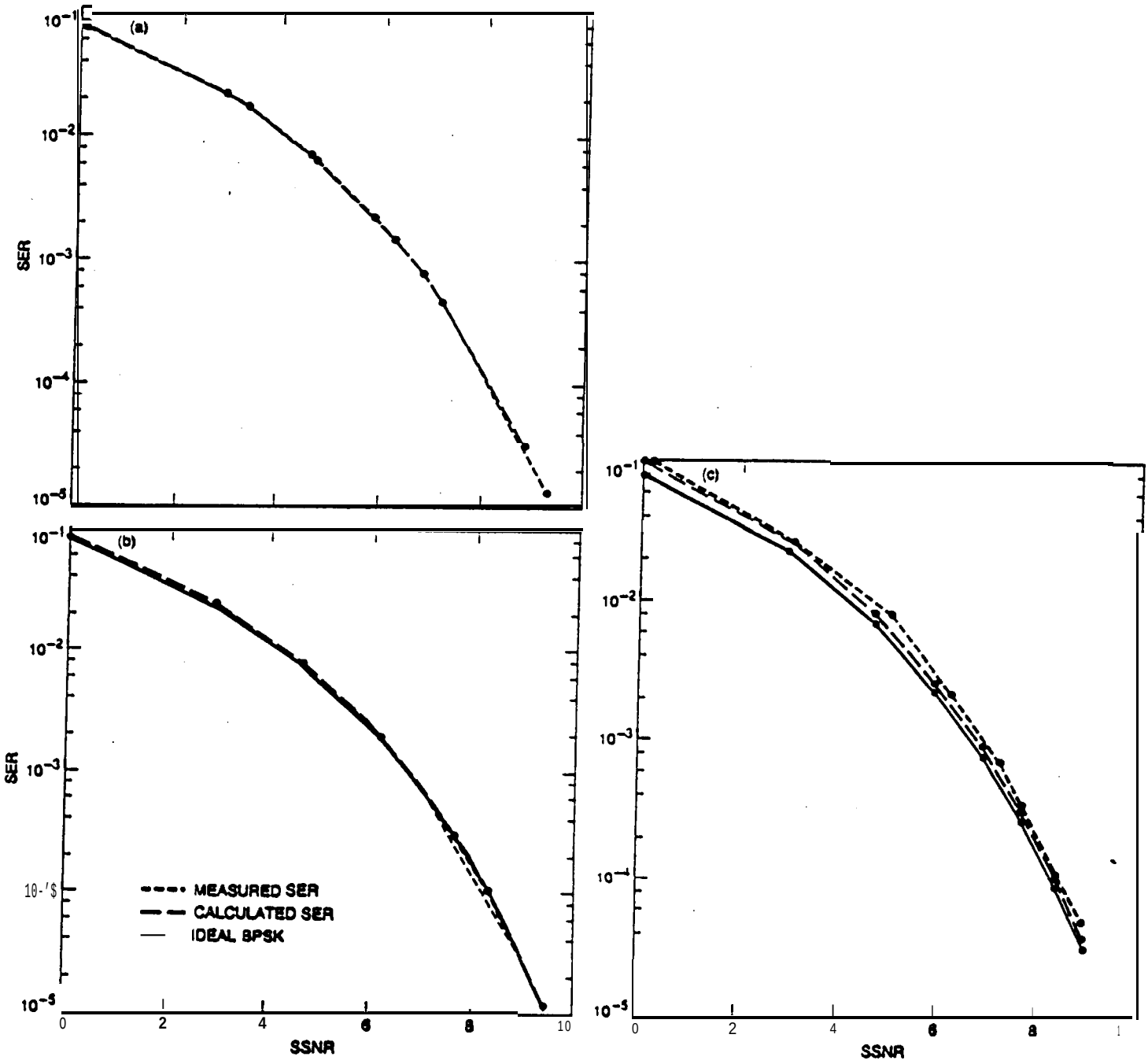

Fig. 1S. Measured performance for PCM/PM/bi-phase: (a) ICR = −39.5 dB (*m* = 1.1 rad, 7 = 0.001); (b) ICR = −34.2 dB (*m* = 1.3 rad, 7 = 0.001); and (c) ICR = −40.2 dB (*m* = 1.3 rad, 7 = 0.00S),

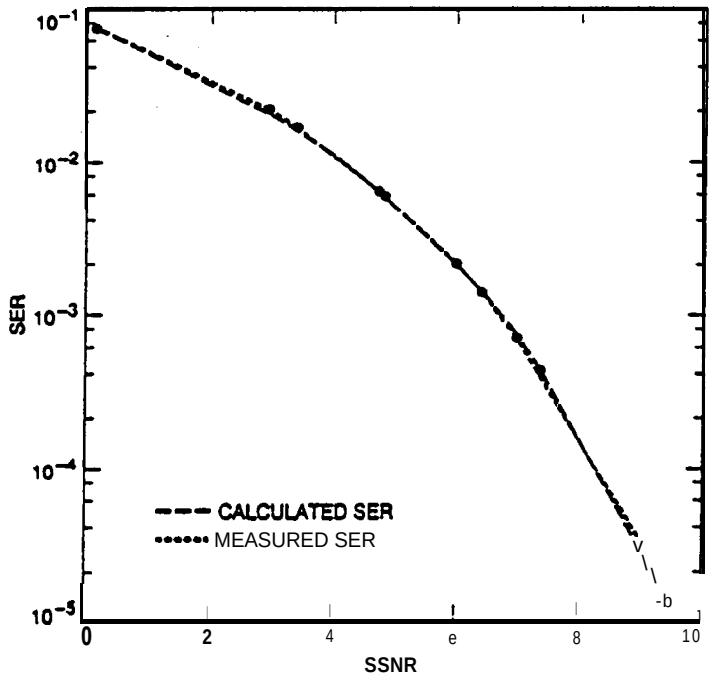

Fig. 16. Measured SER for PCM/PSK/PM with square-wave subcarrier, $m = 1.1$ rad and $\gamma = 0.001$.